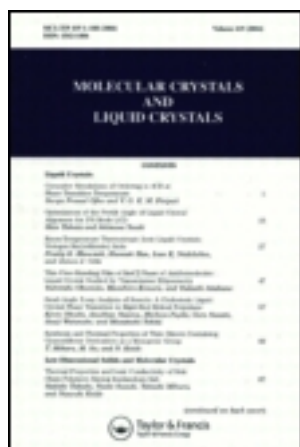


Informa Ltd Registered in England and Wales Registered Number: 1072954 Registered office: Mortimer House, 37-41 Mortimer Street, London W1T 3JH, UK



Version of record first published: 24 Sep 2006.

The publisher does not give any warranty express or implied or make any representation that the contents will be complete or accurate or up to date. The accuracy of any instructions, formulae, and drug doses should be independently verified with primary sources. The publisher shall not be liable for any loss, actions,

claims, proceedings, demand, or costs or damages whatsoever or howsoever caused arising directly or indirectly in connection with or arising out of the use of this material.

## A STUDY OF THE GLASS TRANSITION IN POLYMERIC MESOPHASES VIA CALORIMETRIC AND NON-LINEAR ESR TECHNIQUES

L. ANDREOZZI, M. GIORDANO, D. LEPORINI, M. MARTINELLI

Dipartimento di Fisica dell'Università, Pisa ITALY

M. PACI

Dipartimento di Ingegneria Chimica, Chimica Industriale e Scienza dei Materiali  
Pisa, ITALY

A. S. ANGELONI

Dipartimento di Chimica Industriale e dei Materiali, Bologna ITALY

(Received March 12, 1991)

**Abstract** In undercooled polymeric mesophases, being annealed at a temperature higher than  $T_g$ , nucleation and crystal growth processes take place. We investigate the ageing of comb-like polyacrilates both by calorimetry and non-linear ESR. After annealing, the local transport properties of the polymers with quenched disorder exhibit relevant changes which are interpreted in terms of a decreased cooperativity of the amorphous part.

**Keywords:** glass transition; non-linear ESR, thermal analysis

### INTRODUCTION

Generally, substances are more stable in crystalline than in glassy state<sup>1</sup>. However, if the material is cooled below  $T_g$  at a rate faster than its own rearrangement time-scales, it is frozen in a metastable configuration with an energy being higher than the crystalline ground-state. The escape time from the potential well where the system is trapped can be extremely long and in this sense the glass transition is viewed as a transition to a non-ergodic state.<sup>2</sup> As a consequence, crystallization can be extremely slowed down. This phenomenon relaxes in polymeric mesophases where mesogenic moieties force a phase ordering which is antagonistic to the glass-forming tendency, strongly driven by the long, flexible backbone. To date, the theoretical study of the interplay between the backbone entropy and the order of the mesogenic units is well developed, especially for comb-like polymers in equilibrium condition<sup>3</sup> but only a few studies by neutron<sup>4</sup> and X-ray<sup>5</sup> scattering concerning the equilibrium conformation in the ergodic state above  $T_g$  have been reported.

The above issues motivated a study aimed to investigate to what extent in glassy polymeric mesophases crystallization is hampered.

We present first results concerning comb-like polymeric mesophases which have been investigated by using Differential Scanning Calorimetry (DSC) and non-linear Electron Spin Resonance (ESR) spectroscopy. The main outcome of the present study is twofold. It will be shown that non-linear ESR, even if it is a local technique, nevertheless is able to expose cooperative effects. Furthermore, evidence will be given of marked changes in the local transport when the amorphous phase is annealed in

the undercooling region. A tentative explanation will be given in terms of a reduced cooperativity in the amorphous matrix due to the pervasive growth of the crystal.

### NON-LINEAR ESR

Being polymers diamagnetic in nature, stable radicals have to be solved as spin probes in the host matrix.<sup>6</sup> ESR spectroscopies are sensitive to probe reorientation, which in polymers usually takes place with a correlation time  $\tau_c > 10^{-8}$  s. In this regime the standard methodologies are faced with the large computational effort which is usually required in order to extract reliable information. However, recently non-linear ESR techniques have provided insight in a more direct way.<sup>7</sup> In particular, due to its high sensitivity to slow dynamics, the Longitudinally Detected ESR ( LODESR ) has attracted our attention. The block scheme of the LODESR spectrometer is sketched in Figure 1. Two microwave fields ( depicted as double arrows in Figure 1 ) with angular frequencies  $\omega_1$  and  $\omega_2$  and amplitudes  $H_1$  and  $H_2$  respectively, both  $\sigma$ -polarized with respect to the applied static magnetic field  $H_0$ , are acted upon the sample  $S$  in resonance condition (  $\omega_1, \omega_2 \approx \omega_0 = \gamma H_0$ ,  $\gamma$  being the magnetogyric factor). The LODESR spectroscopy deals with the signal induced on the coil  $C$  by the component of magnetization parallel to  $H_0$  oscillating at  $\Delta = |\omega_1 - \omega_2|$  and harmonics.

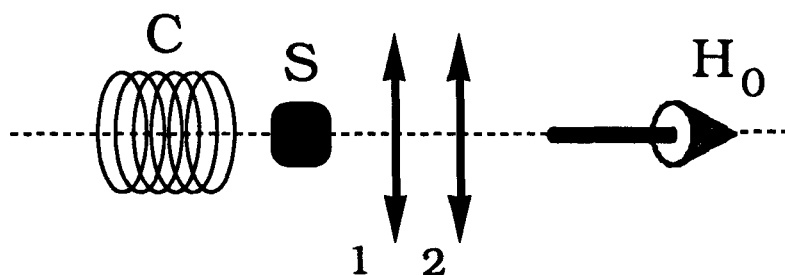


FIGURE 1 Block scheme of the LODESR spectrometer. See text for details

Different operating modes can be devised. Here, we refer to the so called frequency-swept mode which detects the signal by sweeping the offset  $\Delta$  between the two waves, being  $H_0$  constant. The frequency-swept LODESR lineshape is governed by longitudinal relaxation processes. This occurrence has been proven to disclose a shortcut to the interpretation. In particular, the familiar case of the nitroxide probes, namely one spin  $S = 1/2$  interacting with a single nuclear spin  $I = 1$  can be recast so as to relate it to a fictitious  $S = 1/2$  spin system. For inhomogeneous lines the amplitude of the signal  $\bar{S}(\omega_1 - \omega_2)$ , after averaging over the distribution of Larmor frequencies can be written as:<sup>7</sup>

$$\overline{S}(\omega_1 - \omega_2) = \overline{I}(\omega_1; \omega_2) \frac{T_1^*}{\sqrt{[(\omega_1 - \omega_2)T_1^*]^2 + 1}} \quad (1)$$

$T_1^*$  is a constant and  $\overline{I}(\omega_1; \omega_2)$  is a function of both  $\omega_1$  and  $\omega_2$ . It can be seen that if the motion of the probe slows down, the term  $\overline{I}(\omega_1; \omega_2)$  weakly depends upon both  $\omega_1$  and  $\omega_2$ . Therefore, by changing  $\Delta = |\omega_1 - \omega_2|$  one yields a lineshape with FWHM equal to  $\sqrt{3}/T_1^*$ . This width is a sensitive parameter of the probe dynamics and, in a sense, the resonating term of Eq. (1) works just as a "quantum filter" of the inhomogeneous broadening of the line.  $T_1^*$  turns out to be simply expressed as:

$$T_1^{*-1} = 6 \langle \Delta H^2 \rangle J(\omega_0) \cong 6 \frac{\langle \Delta H^2 \rangle}{\omega_0^2} \frac{1}{\tau_c} \quad (2)$$

where  $J(\omega_0)$  is the spectral density at  $\omega_0$  of the fluctuating magnetic fields, acting on the spin system with average squared amplitude  $\langle \Delta H^2 \rangle^{1/2}$ . The exact form of  $J(\omega_0)$  depends on the specific model assumed for the motion of the probe. In Eq. (2) a free diffusion has been assumed in the limit  $\omega_0 \tau_c \gg 1$ , which is well matched.

## EXPERIMENTAL

### Sample

The material under investigation is the *side-chain* polymer Poly[[ 4-Pentiloxo-3'-methyl-4'-(6-acryloxyxyloxy)] azobenzene] (Figure 2), which hereafter will be

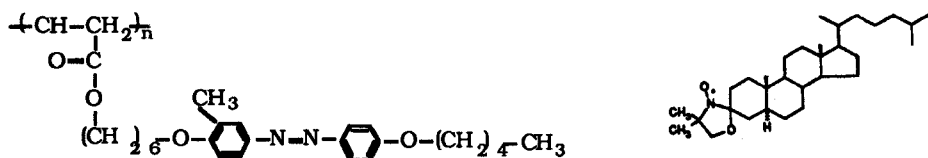


FIGURE 2 Left side: structure of PA. Right side: structure of the cholestane probe

referred to by the acronym PA.<sup>8</sup> The macromolecule belongs to the polyacrilate class, with average molecular weight  $\overline{MW} = 15000$ , which corresponds to about 40 monomers and is almost monodisperse. The glass transition temperature  $T_g$  was found at 293 K. No other transitions were found by cooling down to temperatures as low as 150 K. Melting of the crystal occurs at  $T_m = 353$  K. According to X-ray diffractometry the ordered phase at temperatures over  $T_m$  is nematic. By examining under microscope (polarizing microscope Leitz Ortholux II attached to a programmable heating stage Mettler FP5 and FP52) thin films of PA, at temperatures over  $T_m$  a reddish, grainy texture (Figure 3) is observed. We remark that the group  $N=N$ , differently from the customary group  $-COO-$ , makes the overall shape of the mesogenic moieties much similar to rods, so making more reliable any comparison with existing theories which

often assume this limiting form. Isotropization of the phase sets in at 365 K.

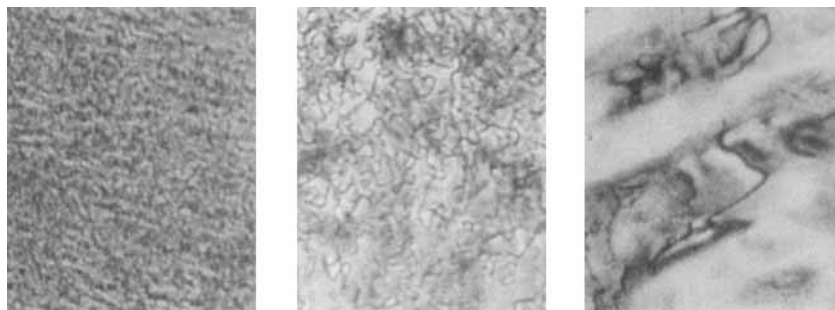


FIGURE 3 Textures of PA. Left: oriented sample ( $\times 140T = 323\text{ K}$ ). Center: unoriented sample ( $\times 140T = 354\text{ K}$ ). Right: unoriented sample ( $\times 410T = 354\text{ K}$ ). See Color Plate II

#### Differential Scanning Calorimetry

Differential scanning calorimetry data were collected using a Perkin-Elmer DSC-4 calorimeter equipped with a 3600 Data Station and Intracooler I; the calorimeter operated with a stream of nitrogen flowing over the sample at a rate of 25 cc/min. Sample weights were in the range of 6-8 mg and indium was used for calibration. The range of temperatures between -40 and +105 K was investigated.

#### Non-linear ESR

The temperature control system is home-built and ensures both an absolute precision of  $10^{-2}\text{ K}$  and a stability of  $10^{-3}\text{ K}$ . Small amounts of the cholestane probe (Figure 2) were solved in the polymeric host, the molar ratio monomer/spin probe being  $10^{-2}$ . The LODSR spectrometer works at 10 GHz and is detailed elsewhere.<sup>7</sup>

### RESULTS AND DISCUSSION

#### Differential Scanning Calorimetry

The polymer, as obtained from precipitation into methanol, shows (Figure 4, curve *a*) two endothermic transitions, peaking at 347 K and 363 K; a second order transition appears at about 297 K. The cooling trace (curve *b*) shows a single exotherm at 357 K, plus the second order transition at about 291 K. During the subsequent heating run (*c*) only one endothermic peak at 365 K is observed. No change of this behaviour takes place if the sample is quenched from the melt at the nominal highest rate available ( $320\text{ K/min}$ ) (curve *d*). On the contrary the samples that had been cooled at lower cooling rates ( $1$  and  $0.1\text{ K/min}$ ) show two endotherms at 350 K and 365 K (curves *e* and *f*, respectively). Furthermore it is observed that the lower is the cooling rate, the higher is the enthalpy associated with the low temperature peak. This peak may be attributed to the fusion of the solid crystalline polymer on the basis of

microscopic observation. In fact, the polymer samples characterized by this endotherm have been shown to acquire fluidity in correspondence with this transition, whereas those which have not such endotherm (samples cooled from the melt at  $20\text{--}320\text{ K/mtn}$ ) already flow at temperatures higher than  $T_g$ . The orientational order is lost in correspondence with the higher temperature transition (isotropization,  $364\text{ K}$ ). The formation of a crystalline phase from the mesomorphic

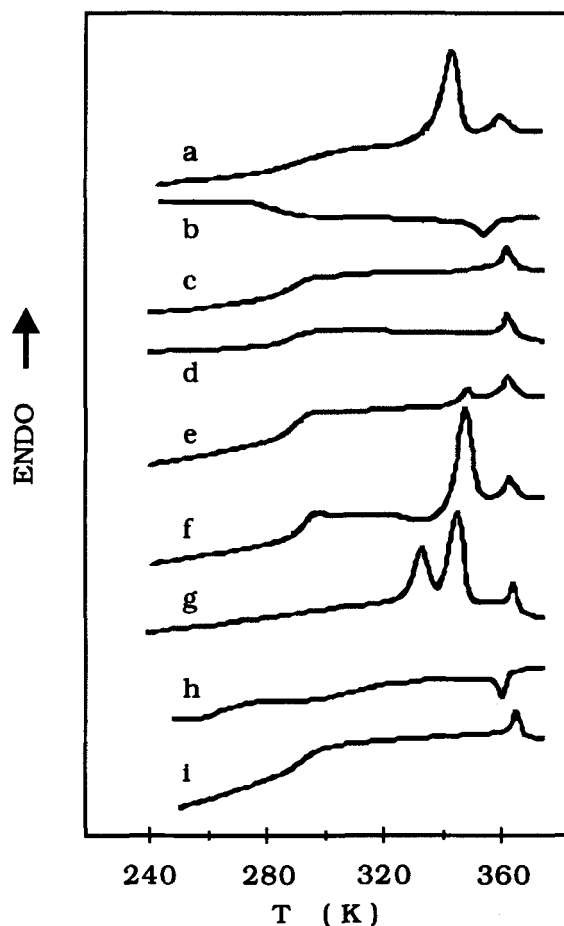


FIGURE 4 DSC traces of PA. See text for details

state seems to be affected by the cooling rate; actually, the crystallization can be realized only by a very slow cooling rate from the melt. To investigate further the crystallization and melting behaviour of this polymer, a quenched sample was annealed for about 30 days at  $300\text{ K}$ , and then examined by DSC. The heating trace (curve g) shows the absence of the glass transition and three endotherms at  $333\text{ K}$ ,  $348\text{ K}$  and  $368\text{ K}$ . This complex behaviour may be explained assuming that an imperfect crystal structure is developed during the low temperature annealing. This

crystalline phase melts, during the heating cycle, in correspondence with the lower temperature peak (333 K) and reorganizes into a more perfect crystalline phase, similar to that obtained by slow cooling from the isotropic state, which finally melts at 348 K. The cooling trace (h) and the subsequent heating trace (i) are identical to the previous ones (curves c and d), thus proving that the thermal treatments do not alter the chemical structure of the polymer.

### Non-linear ESR

Results concerning the amorphous phase of PA were published elsewhere.<sup>7</sup> For readers' convenience we touch on the main conclusions. In Figure 5 the plot of the observed temperature dependence of  $1/T_1^*$  is shown.

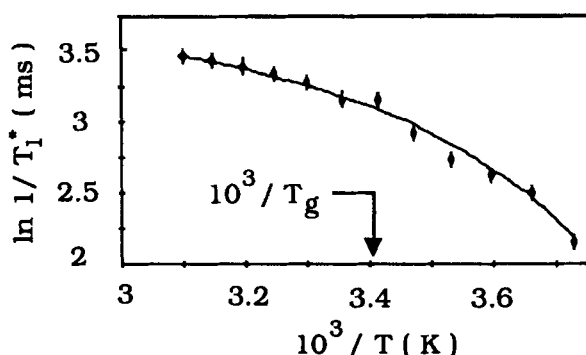


FIGURE 5 Temperature dependence of  $1/T_1^*$  for the cholestane probe in the amorphous phase of PA. The error bars correspond to a 5% of relative uncertainty. The superimposed curve is the best-fit result according to Eq. 3 with  $T_g - T_0 = 55$  K.

The scan extends across the zone of transition to the amorphous phase, marked loosely by the value  $T_g$ . The overall trend of Figure 5 is well described by the trial function:

$$\frac{1}{T_1^*} = A \exp\left(-\frac{b}{T - T_0}\right) \quad (3)$$

In view of Eq. (2), basis to Eq. (3) is provided by recalling that in a number of glass-forming materials the temperature dependence of the correlation time for a particle moving in an amorphous cluster is well described by a law of the Williams-Landel-Ferry (WLF) form, i.e.  $\tau_c = \tau_\infty \exp[b/(T - T_0)]$  where  $b$  and  $\tau_\infty$  are positive constants and  $T_0$  is the Kauzmann temperature.<sup>2</sup> The best-fit value  $T_g - T_0 = 55$  K is close to the average value  $T_g - T_0 \approx 51.6$  K, being found for the great majority of polymeric systems. We also find  $b = 120$  K, smaller than the average value of about 800 K for polymers, corresponding to a fragility  $D \equiv b/T_0 = 0.5$ . However, differently from  $T_0$ , only depending on the host matrix, the parameter  $b$  is affected by probe-polymer

interactions, which are not so strong due to voids in the amorphous structure where the guest probe fits well.

The spin relaxation, being detected by LODESR, exhibits significant changes after annealing a quenched sample of PA. The Arrhenius plot of  $T_1^*$  for a sample annealed at 300 K during a period of ten days is shown in Figure 6.

By increasing the temperature, at  $T_g$  a strong decrease of  $T_1^*$  and then of  $\tau_c$  is observed. By using Eq. (2), at  $T = 300$  K one estimates  $\tau_c \approx 10^{-7}$  s, a value being confirmed by ESR simulations. We conclude that, during the annealing, which occurs at a temperature a little higher than  $T_g$ , the sample has not reached the thermal equilibrium state, but at a temperature above  $T_g$  the structure fully unfreezes and tends to recover the proper equilibrium configuration. A similar strong reorganization has

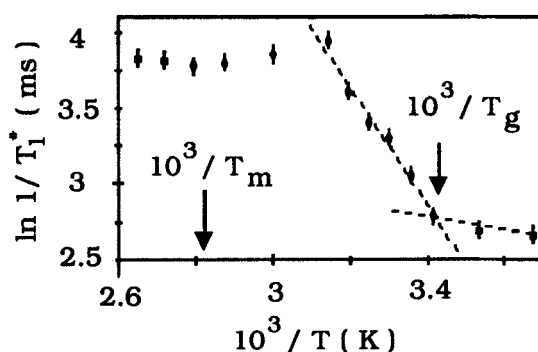


FIGURE 6 Temperature dependence of  $1/T_1^*$  for the cholestane probe in the annealed phase of PA. The error bars correspond to a 5% of relative uncertainty. The lines are guides for the eye. Their slope correspond to apparent activation energies of 8.8 KCal/mole and 0.8 KCal/mole.

been already observed in polymeric mesophases. Both F.Moussa *et al.* and F.Hardouin *et al.* have detected in side-chain polymethacrylates just above  $T_g$  a strong coil-up of the backbone along the direction normal to the alignment of the mesogens.<sup>4</sup> It was also observed that the parallel dimension of the backbone was nearly unaffected by crossing  $T_g$ . This process is little dependent on the ordered phase reached at equilibrium above  $T_g$ , since has been observed both in nematic and smectic mesophases. In the nematic sample the apparent activation energy is comparable (about 7.9 KCal/mole) to the one observed in PA. This coincidence is appealing but definitely not conclusive, since similar activation energies are also found both for spin probes<sup>9</sup> and other impurities<sup>10</sup> in nematics. At higher temperatures a new regime sets in where a weak temperature dependence of  $T_1^*$  is observed. In this interval the melting of the crystalline portion of the sample takes place, so leading to a nematic melt. The large structural rearrangements occurring at  $T_m$  are only weakly signaled by LODESR. It is given to believe that the spin probe is segregated in the amorphous part of the sample, still surviving near  $T_m$ . In fact, we can argue that the amorphous matrix is just organized like a nearly frozen nematic and therefore only limited effects are expected to affect the probe at  $T_m$ . Moreover, the expulsion of large spin probes (such

as the cholestane probe ) from highly packed zones is a well known phenomenon, which has been already observed in ordinary liquid crystals.<sup>9</sup>

In light of the above discussion, a comment on the different trends occurring at  $T_g$  in the annealed and amorphous sample respectively seems appropriate. The Williams-Landau-Ferry law observed in amorphous samples is a consequence of the cooperativity occurring in the disordered matrix.<sup>2</sup> This is signaled by large apparent activation energies at low temperature. Crystalline clusters decrease the cooperativity, by constraining the overall structure. As a consequence, local transport properties are locally driven. Figure 6 reflects this new regime, being the low temperature behaviour of  $\tau_c$  governed by a lower activation energy. The behaviour detected by LODESR is intermediate between the amorphous case ( Figure 4 curves c and d , Figure 5 ) and the highly crystallized case ( Figure 4 curve g ), being the crystal growth sufficiently high so as to affect the collective character of the amorphous structural relaxation.

## CONCLUSIONS

In this communication a first report has been given of a study aimed at investigating the competition existing in polymeric mesophases between glass-forming and crystallization tendencies. In the side chain polymers under discussion calorimetry points out that effecting a compromise takes some weeks. It is proven that a local technique such as the ESR spectroscopy can provide insight into the non-local character of the transport properties. In particular, non linear ESR techniques are able to characterize different degrees of the cooperativity governing the relaxation of amorphous structure.

## REFERENCES

1. A.R.Ubbelohde, The Molten State of Matter ( Wiley, New York 1978 ).
2. D.Richter, T.Springer eds. , Polymer Motion in Dense Systems ( Springer, Berlin 1988 ); D.Richter, A.J.Dianoux, W.Petry, J.Teixeira eds., Dynamics of Disordered Materials ( Springer, Berlin 1989 ).
3. W.Renz, M.Warner, Proc.R.Soc.Lond.A, **417**, 213 ( 1988 ); J.Rieger, J.Phys (France), **49**, 1615 ( 1988 ); F.Dowell, Mol.Cryst.Liq.Cryst. **157**, 203 ( 1988 ).
4. F.Moussa, J.P.Cotton, F.Hardouin, P.Keller, M.Lambert, G.Pepy, M.Mauzac, H.Richard J.Phys (France), **48**, 1079 ( 1987 ); F.Hardouin, L.Noirez, P.Keller, M.Lambert, F.Moussa, G.Pepy, Mol.Cryst.Liq.Cryst **155**, 389 ( 1988 );
5. P.Davidson, P.Keller, A.M.Levelut, J.Phys (France), **46**, 939 ( 1985 ); H.Matoussi, R.Ober, M.Veysse, H.Finkelmann, Europhys.Lett., **2**, 233 ( 1986 ); E.Nachliel, E.N.Keller, D.Davidov, H.Zimmermann, M.Deutsch, Phys.Rev.Lett., **58**, 896 ( 1987 );
6. L.Berliner and J.Reuben eds., Biological Magnetic Resonance Vol.VIII ( Plenum, NY 1989 ).
7. L.Andreozzi, M.Giordano, D.Leporini, M.Martinelli, L.Pardi submitted to Europhys.Lett.
8. A.S.Angeloni, D.Caretti, M.Laus, E.Chiellini, G.Galli, in press on J.Polym.Sci.
9. E.Meirovitch, D.Igner, E.Igner, G.Moro, J.H.Freed, J.Chem.Phys. **77**, 3915 (1982).
10. G.Kruger, Phys.Rep., **82**, 229 ( 1982 ).